NUMERICAL SIMULATION OF FLAME ACCELERATION AND DEFLAGRATION-TO-DETONATION TRANSITION IN HYDROGEN-AIR MIXTURES WITH CONCENTRATION GRADIENTS

Wang, C.J.[1], Wen, J.X.[2*]
[1] School of Civil Engineering, Hefei University of Technology, Hefei, 230009, Anhui, China, chjwang@hfut.edu.cn
[2] Warwick FIRE, School of Engineering, University of Warwick, Coventry CV4 7AL, United Kingdom, jennifer.wen@warwick.ac.uk

ABSTRACT

Flame acceleration in inhomogeneous combustible gas mixture has largely been overlooked despite being relevant to many accidental scenarios. The present study aims to validate our newly developed density-based solver, ExplosionFoam, for flame acceleration and deflagration-to-detonation transition. The solver is based on the open source computational fluid dynamics (CFD) platform OpenFOAM®. For combustion, it uses the hydrogen-air single-step chemistry and the corresponding transport coefficients developed by the authors. Numerical simulations have been conducted for the experimental set up of Ettner et al. [1], which involves flame acceleration and DDT in both homogeneous hydrogen-air mixture as well as an inhomogeneous mixture with concentration gradients in an obstucted channel. The predictions demonstrate good quantitative agreement with the experimental measurements in flame tip position, speed and pressure profiles. Qualitatively, the numerical simulations reproduce well the flame acceleration and DDT phenomena observed in the experiment. The results have shown that in the computed cases, DDT is induced by the interaction of the precursor inert shock wave with the wall close to high hydrogen concentration rather than with the obstacle. Some vortex pairs appear ahead of the flame due to the interaction between the obstacles and the gas flow caused by combustion-induced expansion, but they soon disappear after the flame passes through them. Hydrogen cannot be completely consumed especially in the fuel rich region. This is of additional safety concern as the unburned hydrogen can potentially re-ignite once more fresh air is available in an accidental scenario, causing subsequent explosions.

The results demonstrate the potential of the newly developed density based solver for modelling flame acceleration and DDT in both homogeneous/inhomogeneous hydrogen-air mixture. Further validation needs to be carried out for other mixtures and large-scale cases.

Keywords: hydrogen safety, flame acceleration, deflagration-to-detonation transition, inhomogeneous hydrogen-air mixture

1.0 INTRODUCTION

With gradual diminishing fossil fuel reserves and increasing demand for alternative energy, the energy landscape is gradually shifting from fossil fuel to green or renewable alternative energy resources such as solar, wind, hydroelectric, etc. This change is also driven by the need to reduce pollutions from the combustion of conventional fossil fuels, greenhouse effect and acid rain etc. Hydrogen is seen as a promising clean energy carrier. This in turn requires the associated safety issues to be addressed.

The accidental release of hydrogen into confined or semi-confined enclosures can often lead to a flammable hydrogen-air mixture with concentration gradients. Accidental ignition of this mixture could result in flame acceleration and deflagration-to-detonation transition. This phenomenon was experimentally investigated by Kuznetsov et al. [2,3]. They showed that flame acceleration in mixtures with concentration gradients may be determined by the maximum local hydrogen concentration in semi-confined geometries. Vollmer et al. [4,5], and Boeck et al. [6,7] reported that a strong positive effect of concentration gradients can be found on flame acceleration, especially in a channel without

obstructions. In other words, concentration gradients can result in significantly stronger flame acceleration compared to homogeneous mixtures. Ettner et al. [1,8] developed a density-based code to simulate flame acceleration and DDT process within OpenFOAM® toolbox. Although their grid resolutions were insufficient to resolve the flow details, the predictions showed good agreement in flame tip velocity, position and pressure etc. with the measurements of Vollmer et al. [3,4] and Boeck et al. [5,6]. Apart from these limited investigations, this topic has largely been overlooked its importance to safety concerns in the context of hydrogen energy applications as well as nuclear safety.

The present study is motivated by the above background and takes advantage of a recently modified version of ExplosionFOAM , a density based CFD solver newly developed within the OpenFOAM® toolbox. The numerical predictions were carried out for the experiments of Ettner et al. [1]. Comparison of the key parameters with the data will be presented. In addition, the detailed numerical predictions will be used to gain insight of the phenomena.

2.0 MATHEMATICAL MODELING

2.1 Governing equations

In the process of flame acceleration and DDT, the reactants are assumed to behave as an idea gas together with the products. The flow is governed by the compressible reactive Navier-Stokes equations as written below:

$$\frac{\partial \rho}{\partial t} + \nabla \cdot \left(\rho \vec{U}\right) = 0 \tag{1}$$

$$\frac{\partial \rho \vec{U}}{\partial t} + \nabla \cdot \left(\rho \vec{U}\vec{U}\right) + \nabla \cdot p = \nabla \cdot \tau \tag{2}$$

$$\frac{\partial \rho E}{\partial t} + \nabla \cdot \left(\rho \vec{U} E\right) + \nabla \cdot \left(\vec{U} p\right) = \nabla \cdot \left(\tau \cdot \vec{U}\right) + \nabla \cdot \left(\lambda \nabla T\right) + \nabla \cdot \left(\sum_{k=1}^{NS} \rho D h_k \nabla Y_k\right) \tag{3}$$

$$\frac{\partial \rho Y_k}{\partial t} + \nabla \cdot \left(\rho \vec{U} Y_k\right) = \nabla \cdot \left(\rho D \nabla Y_k\right) + \omega_k \tag{4}$$

where ρ , $\vec{U}$, p , E , and Y_k are the density, velocity, pressure, total internal energy, enthalpy and mass fraction of the ith species, respectively. t is time, τ is stress tensor and NS is species number. The source term, $\overline{\omega}_k$ is chemical reaction production rate. D and λ denote diffusion coefficient and thermal conductivity. Turbulence is simulated using standard k-ε model [9].

2.2 Chemistry model

Ideally full chemistry needs to be used in the DDT simulations. The widely used hydrogen-air chemistry models typically have 9 species and dozens of reactions, e.g. Oran et al. [10] used a scheme with 9 species and 48 reactions, O'Conaire et al. [11] used a scheme with 9 species and 21 reactions. For the simulations of most shock tube tests, the computational mesh would need to be in the order of millions to even tens of million because of the size of the physical domain. It would be computationally too expensive to use detailed kinetic schemes. A single-step chemistry model is a viable alternative approach, which has already been adopted by a number of investigators including the ahthors' groups [12-14]. In this paper, for addressing the chemical source terms in equations (3) and (4), the one step chemistry model developed by Wang et al. [15] was employed for hydrogen-air combustion:

$$H_2 + 0.5O_2 = H_2O \tag{5}$$

The reaction rate in Arrhenius form can be expressed as

$$-\frac{d[H_2]}{dt} = 1.13\times10^{15}\exp\left(\frac{-112957.41}{RT}\right)[H_2][O_2] \tag{6}$$

2.3 Numerical scheme

Within OpenFOAM® toolbox, ExplosionFOAM, a density based CFD solver was developed to solve the above governing equations (1) to (4) using the finite volume method. This solver assembles the famous Godunov type schemes such as Roe [16] and Roe and Pike [17], advection Upstream Splitting Method (AUSM) [18-20] and Harten-Lax-van-Leer_contact (HLLC) [21], etc. For the present study, the HLLC method was used to integrate the convective terms. For time integration, the second-order Crank-Nicholson scheme was adopted. The viscous terms are evaluated with second-order central differencing discretization. The governing equations are then solved using the parallel ExplosionFoam solver with adaptive mesh refinement (AMR). The entire computational domain was initially covered by coarse grids, and along with the computation, fine grids were imposed on the coarse grids in the regions with large temperature gradients. The finest grid is around 1/32 half reaction length, which is sufficient for flame and detonation simulations [22].

3.0 CASE SETUP

Numerical simulations were conducted for the the experimental set up of Ettner et al. [1] for flame acceleration and DDT in hydrogen-air mixture with concentration gradients in an obstucted channel, which is 5.4 m long and 0.06 m high. Seven obstacles with the blockage ratio 60% (BR=2h/H) were mounted on the top and bottom walls. The first obstacle has a distance of 0.25m away from the left ignition end. The obstacle spacing (S) is 300mm. The schematic of the computational domain is shwon in Figure 1. Both homogenous hydrogen-air mixture and mixtures with concentration were considered. The homogeneous mixture has a hydrogen mole fraction 30%. The hydrogen concentration distribution for the inhomogeneous mixture is shown in Figure 2. It should be noted that, as described by Ettner et al. [1], the latter would have an identical homogenous hydrogen mole fraction with the former if it is kept for more than 60 s before ignition to allow for hydrogen and air to mix uniformly. Six probe locations for pressure history are set at distances of 0.5, 1.4, 2.3, 3.1, 4.1 and 5.0 m away from the left end of the channel.

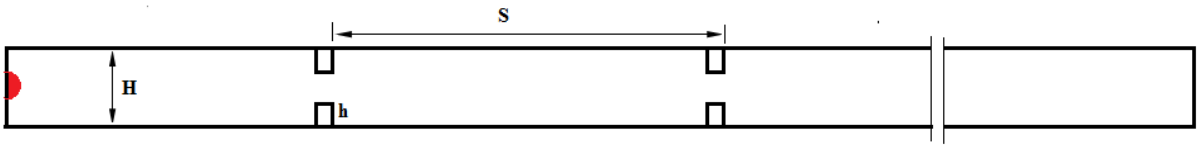

Figure 1. The schematic of the computational domain.

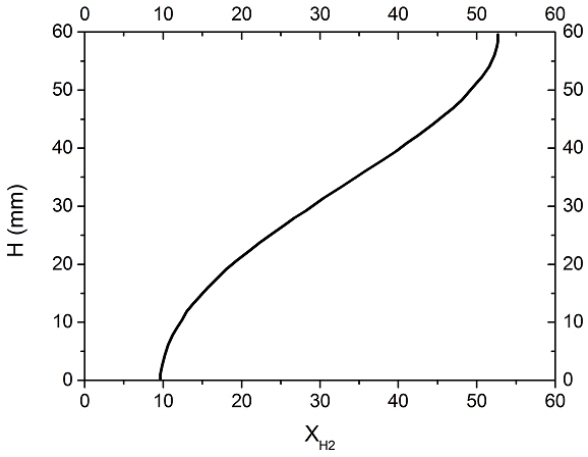

Figure 2. Distribution of the hydrogen mole fraction (30% hydrogen) for the inhomogeneous case.

4.0 RESULTS AND DISCUSSIONS

4.1 The homogenous case

Figure 3 presents the flame tip position X_{tip} as a function of time t while Figure 4 shows the flame tip speed V as a function of flame tip position X_{tip}. Both the predicted flame tip position and speed are in reasonably good agreement with the experimental data. Near the channel entrance when $x < 0.25\,\text{m}$, the flame propagates at a nearly constant laminar speed of around several meters per second. When it diffracts from the first set of obstacles at $x = 0.250\,\text{m}$, the flame speed is abruptly increased, which can be attributed to the amplification of combustion-induced expansion and turbulence generation due to interaction with obstacles [1]. Subsequently, the flame speed continues to increase to around 600m/s almost linearly between the first and second sets of obstacles. When the flame reaches and passes the second set of obstacles, the obstruction resulted in almost 50% reduction of the flame speed over a short distance of around 0.1 m. Following this, the flame speed started to increase steeply, resulting in DDT transition in front or at rear of the third obstacle ($x = 0.85\,\text{m}$). The detonation speed in the experiment exhibited a large fluctuation with the maximum and minimum values of 3600m/s and 730m/s in both the obstructed and non-obstructed sections in the channel. However, the average value is in line with the Chapman-Jouguet (CJ) detonation speed of about 2100 m/s and the predictions.

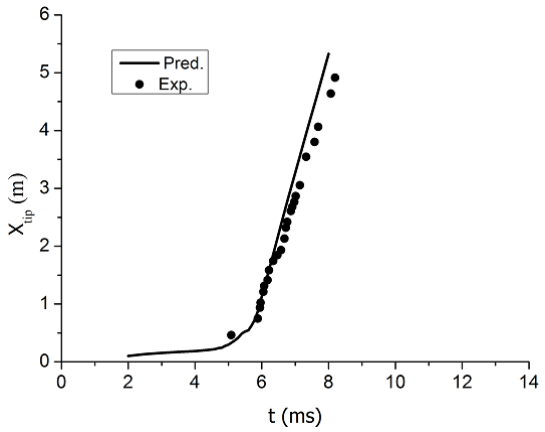

Figure 3. Flame tip position as a function of time in homogeneous hydrogen-air mixture.

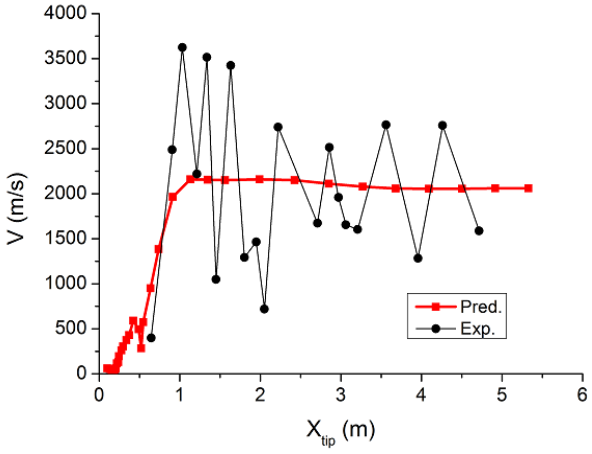

Figure 4. Flame tip speed as a function of flame tip position in homogeneous hydrogen-air mixture.

4.2 The inhomogeneous case with hydrogen concentration gradients

Figure 5 presents flame tip position X_{tip} as a function of time t and Figure 6 illustrates the flame tip speed V as a function of flame tip position X_{tip}. Again reasonably good agreement has been achieved between the predictions and experimental measurements. In particular, the predicted flame tip positions here are in even better agreement with the measurements than that for the homogeneous hydrogen-air mixture. For $x<1.0$ m, the monotonic increase of flame speed can be observed in the experiment. The predicted flame tip speed increases before reaching the first set of obstacles and decelerates over a short distances before increases again towards reaching the 2nd set of obstacles. A short distance of deceleration was also predicted after the flame passed the 2nd set of obstacles. The deceleration can be attributed to the pressure wave which reflects off the obstacle and propagate in the reverse direction and interacts with the flame. This reversely propagating pressure wave has the tendency to push back the flame, resulting in flame deceleration. Such interaction also damps the turbulence level in the mixture. In Figure 6, the fluctuation of the flame tip speed after DDT can also be observed. However, the measured average detonation speed is around 100m/s less than the predicted value.

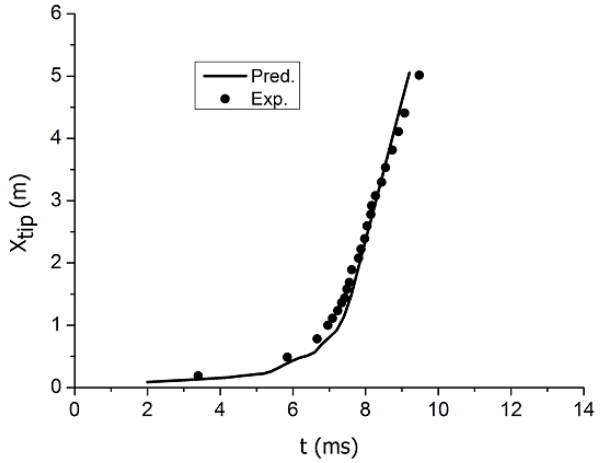

Figure 5. Flame tip position as a function of time in hydrogen-air mixture with concentration gradients.

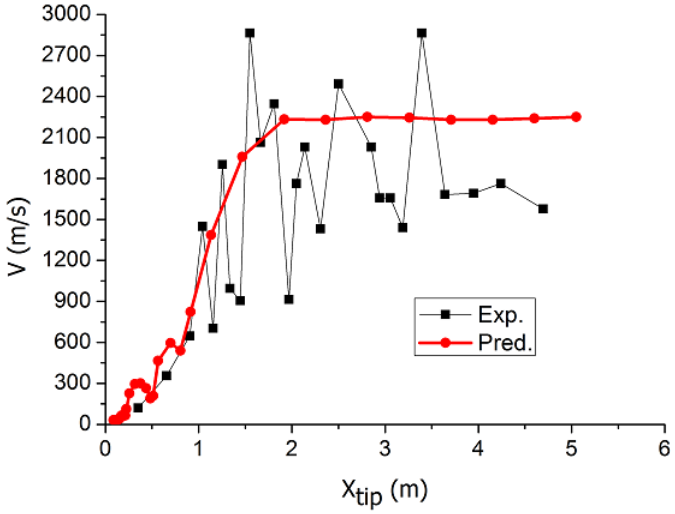

Figure 6. Flame tip speed as a function of flame tip position in hydrogen-air mixture with concentration gradients

Figure 7 presents the predicted pressure profiles at specified probe locations. Overall, the predicted pressure follows the experimental trend and match reasonably well with the measurements quantitatively. Especially, the predicted first peak times at 0.5, 1.4, 2.3 and 3.1m are in good agreement with the measurements. However, the predicted first peak occurrence times at 4.1 and 5.0 m are earlier than the predicted one. Except the peak pressure at 4.1m, all the predicted peak values are slightly smaller than the measured values. Especially, the predicted second peak pressure occurrence times at 2.3, 3.1, 4.1 and 5.0 m are much different from those in experiment.

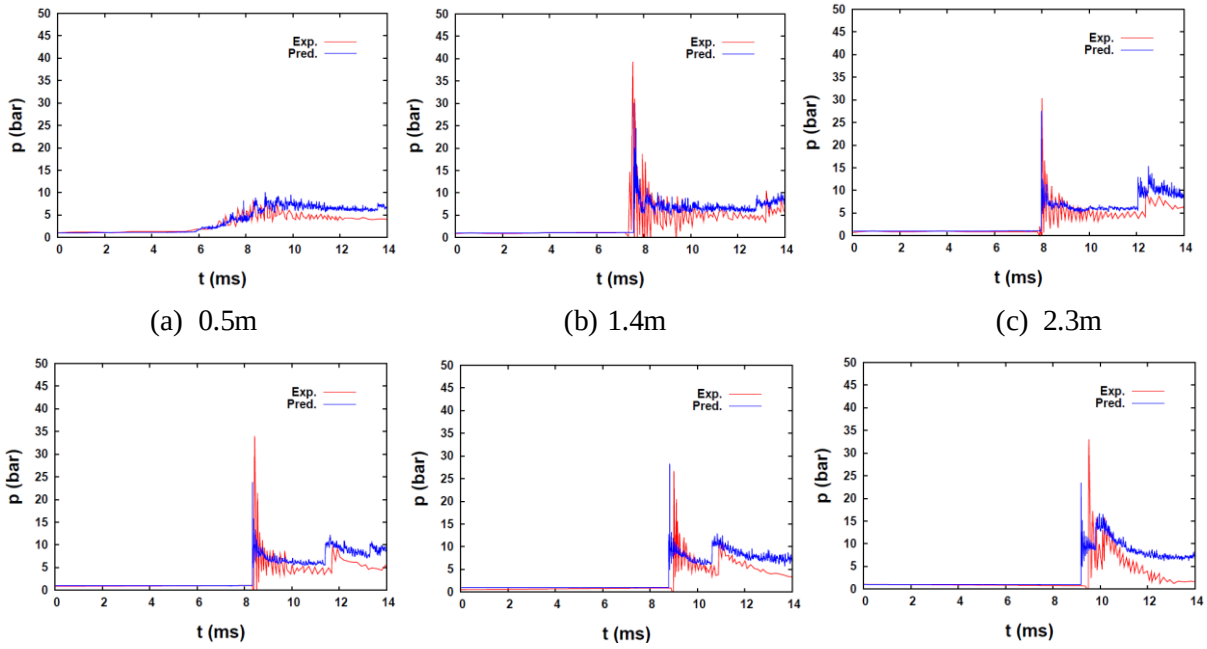

(a) 0.5m (b) 1.4m (c) 2.3m

(d) 3.1m (e) 4.1m (f) 5.0m

Figure 7. Comparison of the predicted and measured pressure profiles at specified probe locations.

4.3 Flame characteristics in hydrogen-air mixture with concentration gradients

Figure 8 shows the predicted temperature, pressure and OH mass fractions during the flame acceleration and DDT. For ease of presentation, the plots only show the sections after the first set of obstacles. At 7.1 ms, the flame is about to interact with the second set of obstacles. A high pressure region can be observed at the left side of it. At 7.2 ms, the flame is passing though the obstacles, a localised high pressure region is generated close to the top wall and a weak shock wave propagates ahead of the flame. At 7.3 ms, a strong curved shock is induced following the weaker wave. Both are regularly reflected back from the bottom wall. At 7.4 ms, the strong shock overtakes the weak shock ahead of it, propagating ahead of the flame. At 7.5 ms, the strong shock wave has interacted with the third set of obstacles, resulting in a relatively strong local explosion, which led to DDT. This process will be examined in more detail later in Figure 9. Following the DDT, the front part of this detonation wave continuously propagates towards the right end and be reflected back from the top wall. The back part meets the reacted mixture and induces a high pressure region by its reflection on the bottom wall. At 7.6 ms, the detonation wave interacts with the fourth set of obstacles. The resulting high pressure leads to the formation of strong multi-reflected shock waves in the downstream region. It should be noted that the vortex pairs can be observed ahead of the flame in the hydrogen concentration fields. They are induced by the interaction of the obstacles and the combustion-induced gas expansion. When the flame passes through these regions, the regular vortex pairs disappear. It is also seen that there are still localised regions with relatively high hydrogen concentrations downstream near the top wall while the relatively low oxygen concentrations there render the mixture to be outside the flammability range. Comparing this with the initial hydrogen concentration distribution in Figure 2, it can be

deduced that in such mixtures with concentration gradients, hydrogen cannot be completely consumed especially in the fuel rich region with hydrogen concentrations higher than the stoichmetric value. This is of additional safety concern as the unburned hydrogen can potentially re-ignite once more fresh air is available in an accidental scenario, causing subsequent explosions.

In order to further analyse the process leading to DDT, Figure 9 zooms in on the temperature and pressure contours. From 7.41 to 7.48ms, the weak shock wave ahead of the flame hits the obstacle and reflects back. The temperature and pressure increase behind the reflected shock wave. But there is no sign of a local ignition. At 7.50 ms after the precursor curved shock wave interacts with the top wall, a significant higher pressure can be observed behind the reflected shock wave. At 7.508 ms, a high temperature region or hot spot appears close to the top wall in the temperature contour. This hot spot is separated from the main flame region. With time elapsing, this spot induces local explosion which transits to detonation as evidenced by the pressure and temperature contours at 7.52 ms. In summary, the DDT results from the precursor shock wave's interaction with top wall and near region with higher hydrogen concentration.

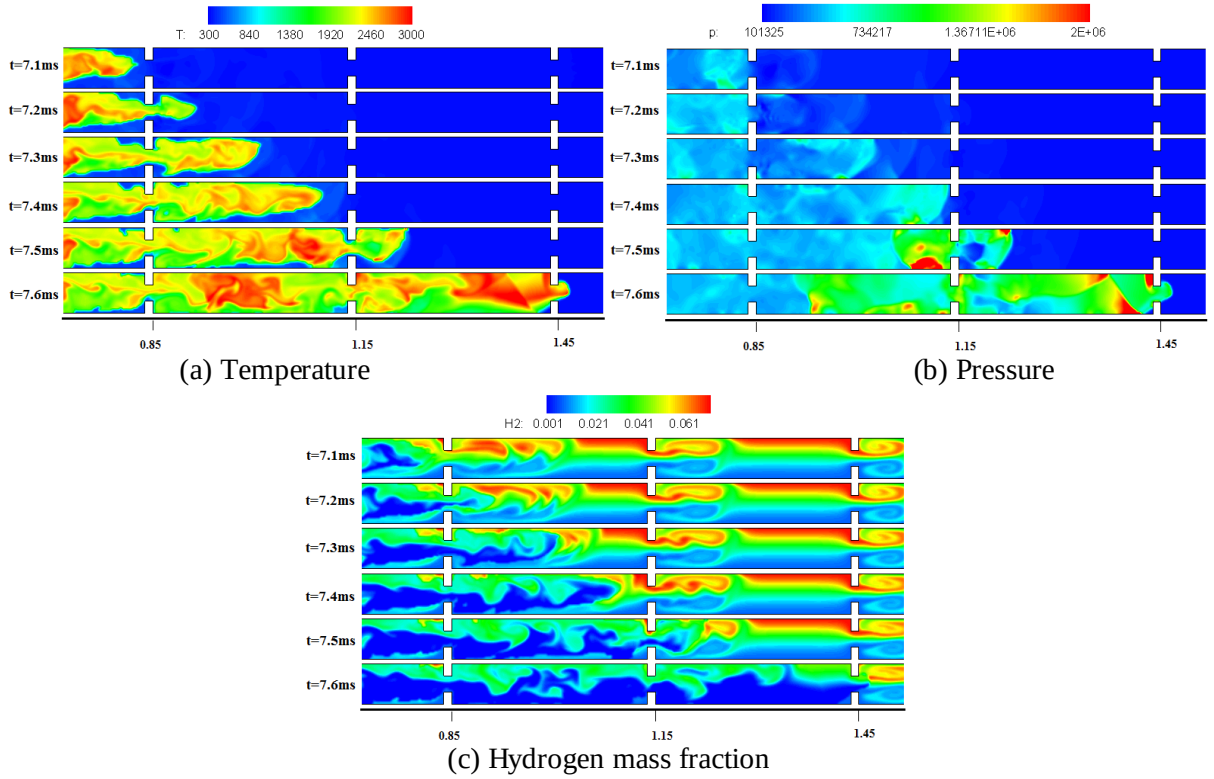

Figure 8. The predicted key parameters during flame acceleration and DDT.

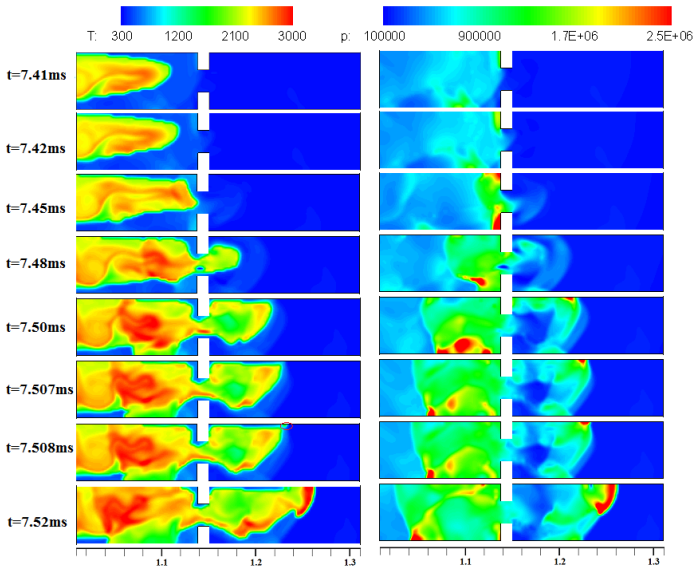

Figure 9. The predicted temperature (left) and pressure (right) contours in the DDT process.

5.0 CONCLUDING REMARKS

ExplosionFoam, a dedicated solver for flame acceleration and DDT has been developed within the frame of the OpenFOAM® toolbox. As part of the validation, the solver has been applied to simulate the experimental set up of Ettner et al. [1], which involves flame acceleration and DDT in both homogeneous hydrogen-air mixture as well as an inhomogeneous mixture with concentration gradients in an obstructed channel. The predictions demonstrate good quantitative agreement with experimental measurements for flame tip position, speed and pressure profiles. Qualitatively, the predictions captured well the flame acceleration and DDT phenomena observed in the experiments.

The analysis has shown that in the present case of hydrogen-air mixture with concentration gradients, the DDT is induced by the interaction of the precursor inert shock wave with the top wall in hydrogen rich region. The shock wave reflects off the top wall, resulting in a hot spot with very high temperature and pressure. Some vortex pairs are generated ahead of the flame due to the interaction between the obstacles and the combustion-induced gas expansion. The results also show that hydrogen cannot be completely consumed especially in the region with hydrogen concentrations higher than the stoichiometric value. This is of additional safety concern as the unburned hydrogen can potentially re-ignite once more fresh air is available in an accidental scenario, causing subsequent explosions.

ACKNOWLEDGEMENTS

The authors gratefully acknowledge the financial support from the National Natural Science Foundation of China (Grant No. 51376174 and 51276177). The research is also partially supported by the return phase funding from the European Commission for the Marie Curie International Fellowships Grant “DETONATION— Advanced numerical study of flame acceleration and detonation in vapour cloud explosions (Grant No. 254658)”.

REFERENCES

1. Ettner, F., Vollmer, K. G., Sattelmayer, T., Numerical Simulation of the Deflagration-to-Detonation Transition in Inhomogeneous Mixtures, *Journal of Combustion*, 2014, pp.1-15.

2. Kuznetsov, M., Grune, J., Friedrich, A., and Jordan, T. , Combustion Regimes in a Stratified Layer of Hydrogen–air Mixture, Proceedings of the International Congress on Advances in Nuclear Power Plants (ICAPP), Nice, France, 2011.
3. Kuznetsov, M., Yanez, J., Grune, J., Friedrich, A., and Jordan, T., Hydrogen combustion in a flat semi-confined layer with respect to the Fukushima Daiichi accident, Proceedings of the International Congress on Advances in Nuclear Power Plants (ICAPP), Chicago. 2012.
4. Vollmer, K.G., Ettner, F., and Sattelmayer, T., Influence of Concentration Gradients on Flame Acceleration in Tubes, *Sci. Technol. Energetic Mater.*, 2011, **72**, pp.74–77.
5. Vollmer, K.G., Ettner, F., and Sattelmayer, T. 2012. Deflagration-to-detonation Transition in Hydrogen-air Mixtures with a Concentration Gradient. *Combust. Sci. Technol.*, 184, 1903–1915.
6. Boeck, L.R., Hasslberger, J., Sattelmayer, T., Flame Acceleration in Hydrogen/Air Mixtures with Concentration Gradients; *Combust. Sci. Technol.*, **186**, No. 10-11, 2014(a), pp. 1650-1661.
7. Boeck, L.R., Msalmi, M., Koehler, F., Hasslberger, J., Sattelmayer, T., Criteria for DDT in Hydrogen-Air Mixtures with Concentration Gradients, 10th International Symposium on Hazards, Prevention and Mitigation of Industrial Explosions, Bergen, Norway, 2014(b).
8. Ettner, F. Effiziente numerische Simulation des Deagrations-Detonations-Übergangs. Ph.D. thesis(in German), Technische Universität München, 2013.
9. Launder B. E. and Spalding D. B., Lectures in Mathematical Models of Turbulence. Academic Press, London, England, 1972.
10. Oran E.S., Young T.R., Boris J.P., Weak and Strong Ignition. I. Numerical Simulations of Shock Tube Experiments, *Combust. Flame*, 1982, **48**, pp. 135–148.
11. O'Conaire, M., Curran, H., Simmie, J., Pitz, W. und Westbrook, C.: A Comprehensive Modeling Study of Hydrogen Oxidation. *International Journal of Chemical Kinetics*, 2004, **36**, pp.603–622.
12. Gamezo V. N., Ogawa T., Oran E. S., Numerical Simulations of Flame Propagation and DDT in Obstructed Channels Filled with Hydrogen-air Mixture. *Proc Combust Institute*, **31,** 2007, pp. 2463–2471.
13. Wang C. J., Wen J. X., Numerical Simulations of Hydrogen-air Detonation Wave Propagation in a Non-uniform Semi-confined Flat Layer, The Sixteenth International Colloquium on Dust Explosions and the Eleventh Colloquium on Gas, Vapour, Liquid and Hybrid Explosions , Bergen, Norway, 2014.
14. Heidari, A., Wen, J.X., Flame Acceleration and Transition from Deflagration to Detonation in Hydrogen Explosions, *International Journal of Hydrogen Energy*, 2014, **39**, pp.6184-6200.
15. Wang C.J., WEN J. X., Lu S.X., Guo J., Single-step Chemistry Model and Transport Coefficient Model for Hydrogen Combustion, *Sci China Tech Sci*, 2012, **55**,pp. 2163-2168.
16. Roe P.L., Approximate Riemann solvers, Parameter Vectors and Shemes. *J. Comput. Phys.* ,1981, **43**(2), pp.357 – 72.
17. Roe P.L., Pike J., Efficient Construction and Utilization of Approximate Riemann Solutions., Proceedings of the sixth international symposium on computing methods in applied sciences and engineering, 1985, 499 – 518.
18. Liou M.S., Steffen Jr CJ. A New Flux Splitting Scheme. *J. Comput. Phys.* ,1993,**107**(1), pp.23 – 39.
19. Liou M.S., A Sequel to AUSM: AUSM+, *J. Comput. Phys*, 1996,**129**(2), pp.364 – 382.
20. Liou M.S., A Sequel to AUSM, part II: AUSM+-up for all Speeds, *J. Comput. Phys*. , 2006, **214**(1), pp.137 – 70.
21. Batten P., Leschziner M.A., Goldberg U.C., Average-state Jacobians and Implicit Methods for Compressible Viscous and Turbulent Flows, *J. Comput. Phys*,. 1997, **137**(1), pp.38 – 78.
22. Sharpe G.J., Quirk J.J., Nonlinear Cellular Dynamics of the Idealized Detonation Model: Regular Cells, *Combustion Theory Modelling*, 2008, **12**, pp.1 - 21.